Supporting Information

Selective Oxidation of Aliphatic Alcohols using Molecular Oxygen at Ambient Temperature: Mixed-Valence Vanadium Oxide Photocatalysts

Sifani Zavahir,[†] Qi Xiao,[†] Sarina Sarina,[†] Jian Zhao,[†] Steven Bottle,[†] Mark Wellard,[†] Jianfeng Jia,[‡] Li-qiang Jing,[§] Yiming Huang,[†] James P. Blinco,[†] Haishun Wu,[‡] and Huai-Yong Zhu*[,†]

[†]School of Chemistry, Physics and Mechanical Engineering, Science and Engineering Faculty, Queensland University of Technology, Brisbane, QLD 4001, Australia

[‡]School of Chemical and Material Science, Shanxi Normal University, Linfen 041004, China

[§]Key Laboratory of Functional Inorganic Material Chemistry, School of Chemistry and Materials Science, Heilongjiang University, Harbin 150080, China

Corresponding Author

*E-mail: hy.zhu@qut.edu.au

Table of content:

Supplementary Figures

Figures S1 to S8

Supplementary Tables

Tables S1 to S3

References

Supplementary Figures

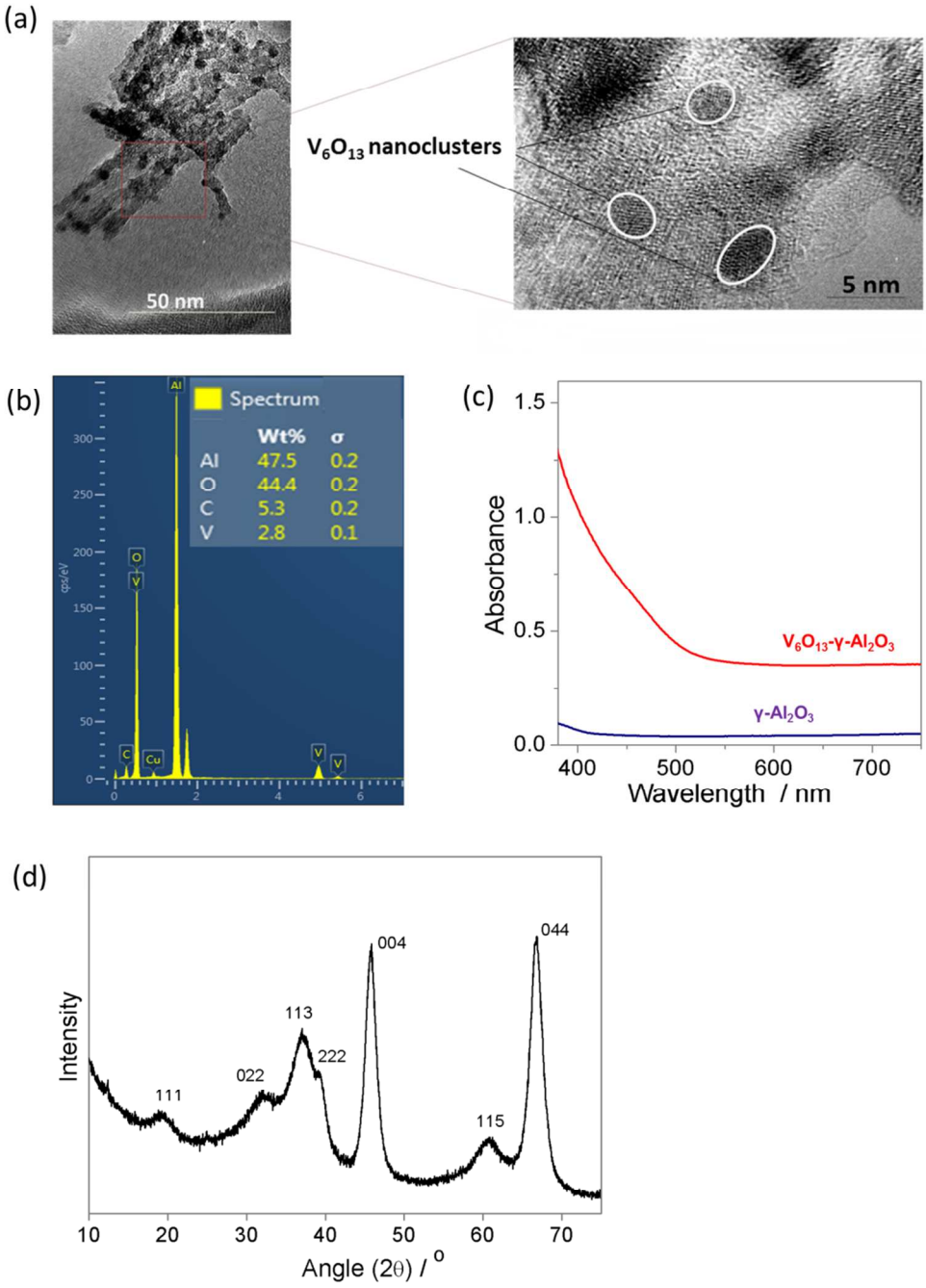

Figure S1. (a) TEM images of the V_6O_{13}-γ-Al_2O_3 sample, (b) elemental composition by EDX analysis of V_6O_{13}-γ-Al_2O_3 sample, (c) UV-Visible diffuse reflectance spectra of the V_6O_{13}-γ-Al_2O_3 sample and pristine γ-Al_2O_3 for comparison, (d) XRD pattern of the V_6O_{13}-γ-Al_2O_3 sample (peaks are indexed for alumina phase).

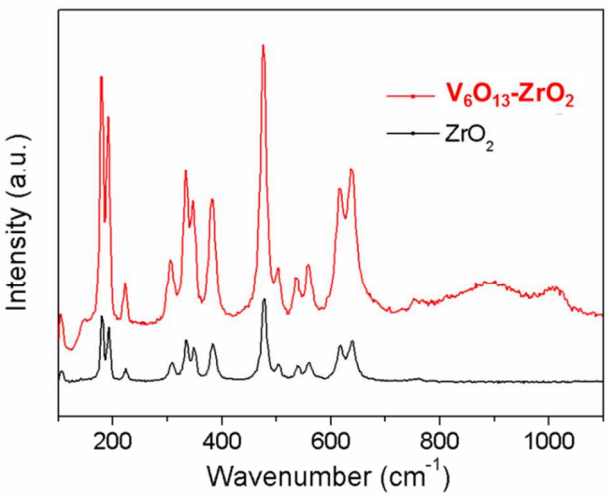

Figure S2. Raman spectra of the V_6O_{13}-ZrO_2 and ZrO_2.

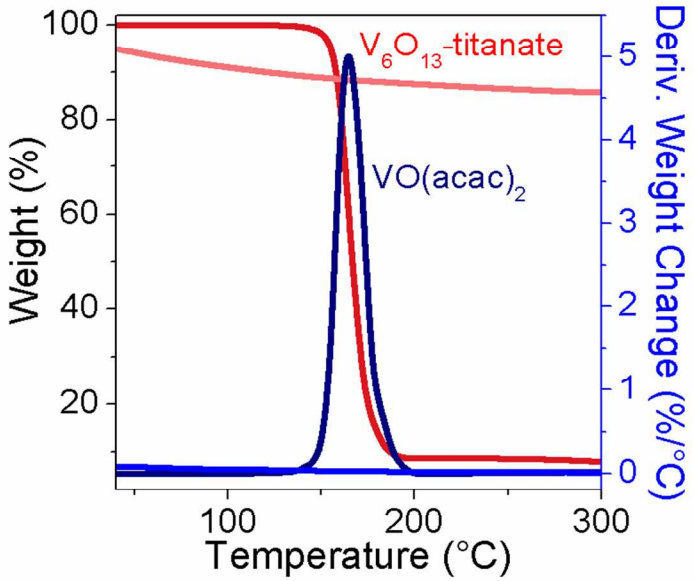

Figure S3. Thermogravimetric analysis data of $VO(acac)_2$ and V_6O_{13}-titanate.

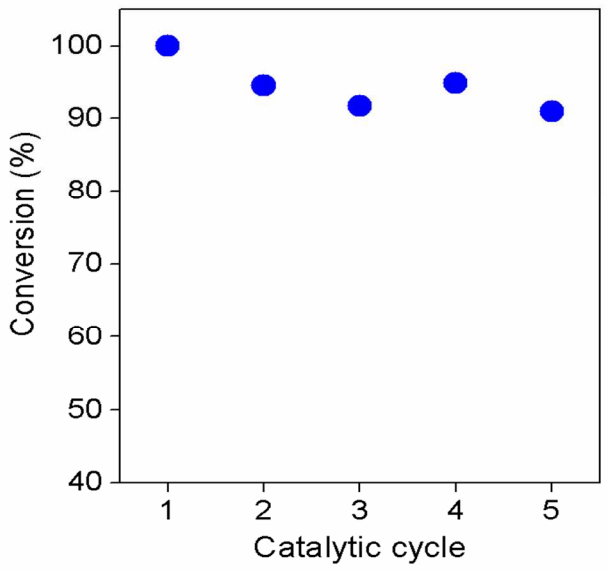

Figure S4. The reusability of catalyst for 3-hexanol oxidation by V_6O_{13}-ZrO_2 catalyst over 5 cycles.

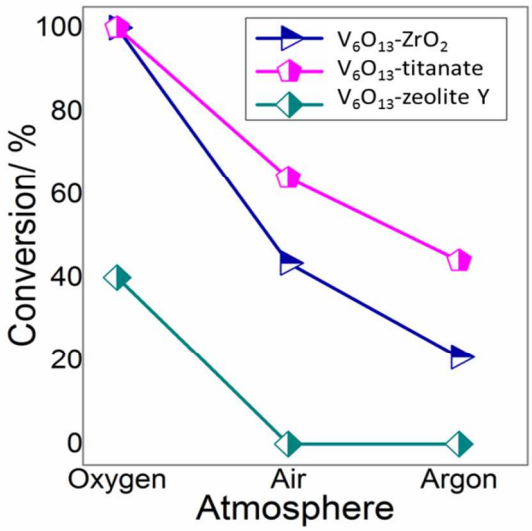

Figure S5. Photocatalytic oxidation of 3-hexanol under different atmospheres.

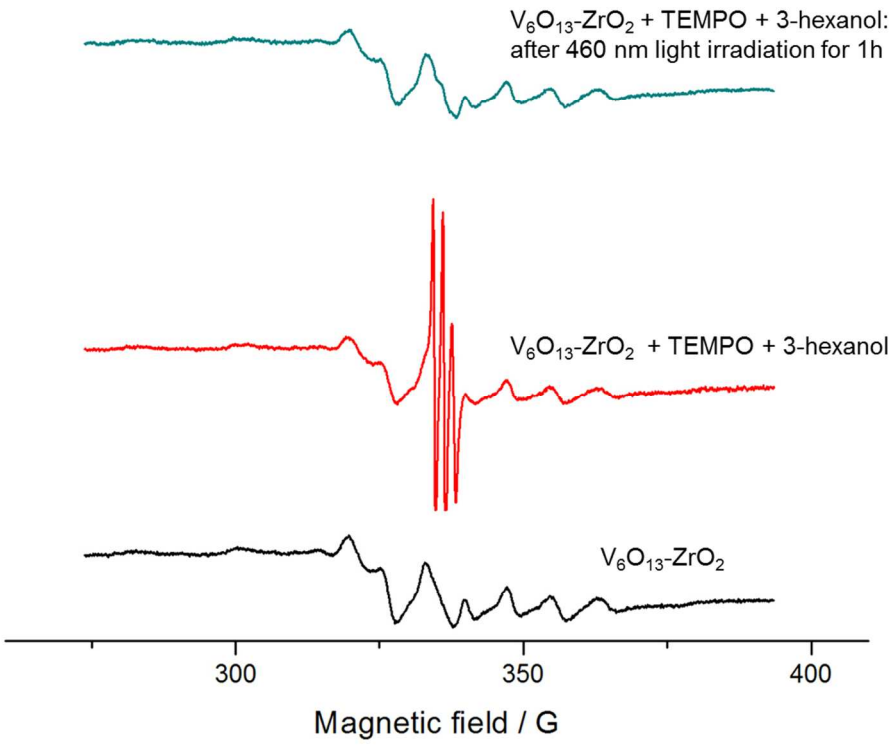

Figure S6. EPR result of the V_6O_{13}-ZrO_2 catalyst.

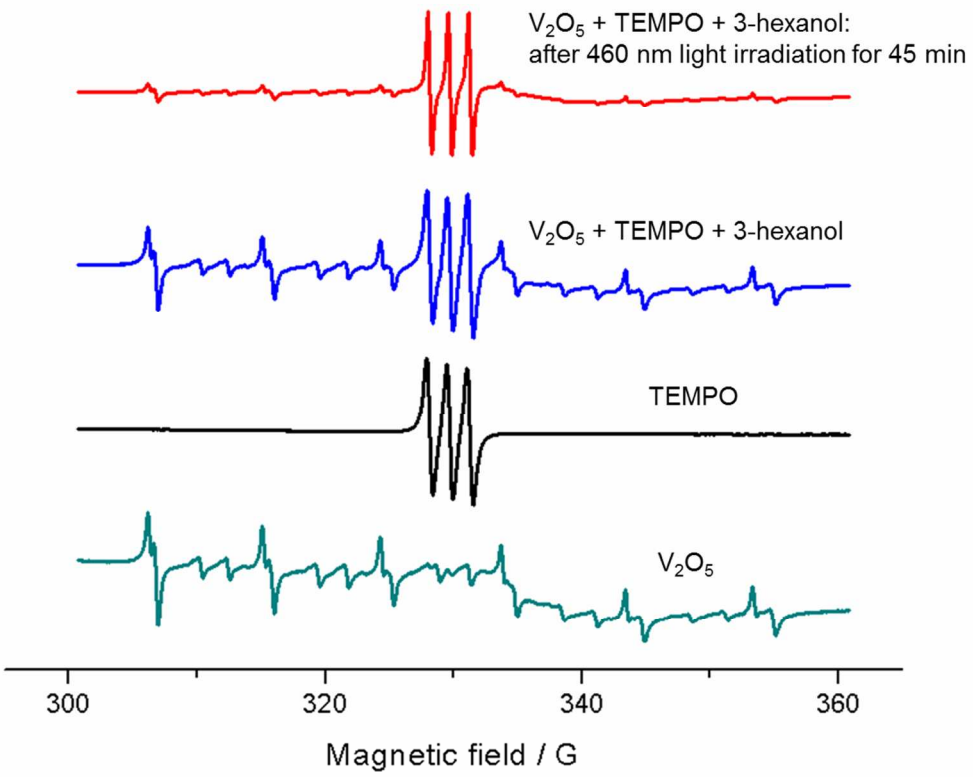

Figure S7. EPR result of the V_2O_5 catalyst.

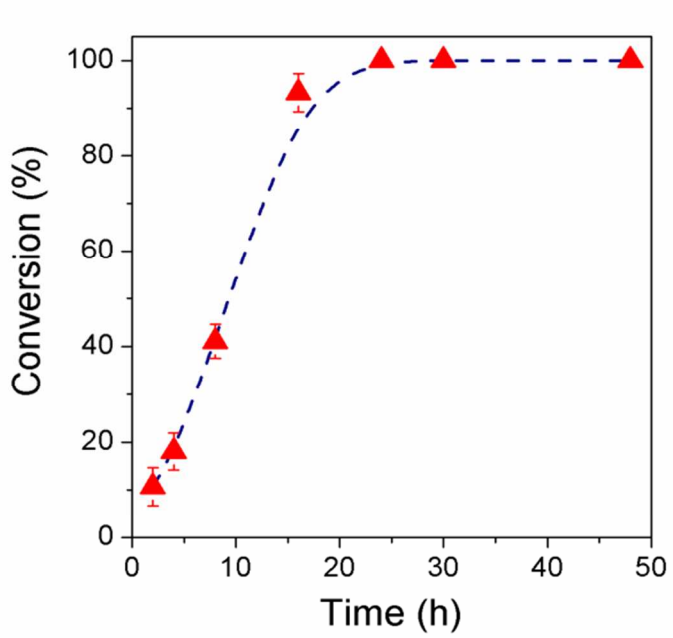

Figure S8. The kinetic study of the oxidation of 3-hexanol using V_6O_{13}-titanate catalyst under visible light irradiation.

Supplementary Tables

Table S1. Comparison of the reaction conditions and achieved conversions of the other catalysts reported in the literature for the oxidation of 3-hexanol to 3-hexanone.

Reference	Reaction conditions	Conversion (%)
1	Cu catalyst, TBHP, 80 °C, 1 h, microwave irradiation (10 W)	57~77
2	Cu catalyst, TBHP, 80 °C, microwave irradiation (10 W power), 240 min	72
3	Oxidovanadium complexes, 80 °C, 2 h 30 min of microwave irradiation (25 W)	28~32
4	$[FeCl_2(Py_2S_2)]$ catalyst, 80 °C, microwave irradiation (10 W power), 240 min	31.7
5	Cu complexes, 120 °C, 0.5 h	48
6	Cu (II) + TEMPO, 80 °C, 0.5 h	42
7	Pd NPs, 85 °C, 15 h	65
Present study	V_6O_{13}-γ-Al_2O_3 or V_6O_{13}-γ-Al_2O_3, 30 °C, 1 atm O_2, 16 h, LED lamp 0.5 W/cm^2	100

Compared with some literature reported reaction conditions of heterogeneous catalysts,[1-7] it can be seen that most of the reported work were conducted under elevated temperatures, while V_6O_{13} catalysts can drive the reaction at only 30 °C with irradiation achieving high conversion (100 %). Thus the V_6O_{13} photocatalyst is much greener and efficient.

Table S2. Influence of excited state quenchers and radical scavengers on the conversion rate of 3-hexanol oxidation to 3-hexanone photocatalysed by V_6O_{13}-ZrO_2[a]

Additive	Activity	V centres / mmol	additive/ mmol	Conv./ %	Select./ %
none	None	0.03	0	100	>99
DTBP	radical scavenger	0.03	0.03	100	>99
pyridine	Excited state quencher	0.03	0.03	51	>99
TEMPO	Excited state quencher/ radical scavenger	0.03	0.03	5	>99

[a] Reaction conditions: 3-hexanol 0.2 mmol; photocatalyst 50 mg; 2 mL of α,α,α-trifluorotoluene; reaction time 16 h; reaction temperature 30 ^{o}C; light source, λ=460 nm LED lamp; light intensity, 0.5 W/cm^2. Vanadium centers were calculated based on vanadium centers available in 50 mg of V_6O_{13} grafted solid according to EDX data.

Table S3. The excited states, corresponding absorption wavelengths and oscillator strengths of V_6O_{13} and adsorption structure of 3-hexanol on V_6O_{13} in the range from 400 to 800 nm.

System		Energy (kcal/mol)	Excited States in visible-light region
V_6O_{13}	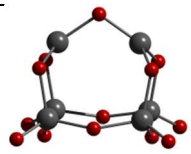	0.0	427.6: 0.0000 436.1: 0.0050 451.0: 0.0000 461.3: 0.0085 484.1: 0.0000 512.1: 0.0009 515.0: 0.0000 522.8: 0.0007 588.5: 0.0000 603.1: 0.0058 649.2: 0.0028 691.5: 0.0003 719.7: 0.0000 730.9: 0.0016
V_6O_{13}-3-hexanol	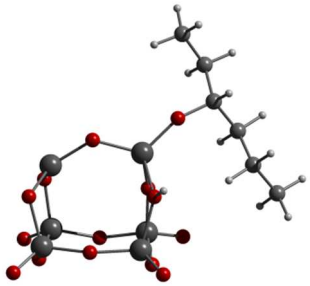	-24.3	404.6: 0.0145 414.4: 0.0015 428.2: 0.0071 442.1: 0.0154 449.2: 0.0015 462.9: 0.0047 468.1: 0.0077 489.1: 0.0230 496.5: 0.0057 515.5: 0.0245 530.1: 0.0011 565.9: 0.0004 595.0: 0.0043 612.8: 0.0026 627.7: 0.0007 664.4: 0.0021 723.8: 0.0008 759.0: 0.0018 774.8: 0.0025

Calculation Method: All the structures were optimized in the framework of density funcational theory (DFT) with the hybrid B3LYP functional.[8] The frequency calculations were carried out to confirm that all the structures are geometrically stable, and to obtain the zero–point vibration energies (ZPE). The energetic term in the text includes the electronic energy and ZPE correction. The optical absorption properties were calculated also with hybrid B3LYP functional in the framework of time-depended DFT (TDDFT).[9] For all the calculations, the standard 6-31++G(d,p) basis set was employed to describe the atomic orbitals of all atoms involved. All the calculations were performed with Gaussian 09 package.[10]

References

1. Nasani, R.; Saha, M.; Mobin, S. M.; Martins, L. M. D. R. S.; Pombeiro, A. J. L.; Kirillov, A. M.; Mukhopadhyay, S. *Dalton Trans.*, **2014**, *43*, 9944–9954.
2. Kopylovich, M. N.; Mizar, A.; Guedes da Silva, M. F. C.; Mac Leod, T. C. O.; Mahmudov, K. T.; Pombeiro, A. J. L. *Chem. Eur. J.*, **2013**, *19*, 588–600.
3. Sutradhar, M.; Martins, L. M. D. R. S.; Guedes da Silva, M. F. C.; Pombeiro, A. J. L. *Appl. Catal., A.* **2015**, *493*, 50–57.
4. Fernandes, R. R.; Lasri, J.; Guedes da Silva, M. F. C.; da Silva, J. A. L.; Fraústo da Silva, J. J. R.; Pombeiro, A. J. L. *Appl. Catal., A.* **2011**, *402*, 110–120.
5. Timokhin, I.; Pettinari, C.; Marchetti, F.; Pettinari, R.; Condello, F.; Galli, S.; Alegria, E. C. B. A.; Martins, L. M. D. R. S.; Pombeiro, A. J. L. *Cryst Growth Des.*, **2015**, *15*, 2303–2317.
6. Sabbatini, A.; Martins, L. M. D. R. S.; Mahmudov, K. T.; Kopylovich, M. N.; Drew, M. G. B.; Pettinari, C.; Pombeiro, A. J. L. *Catal. Commun.,* **2014**, *48*, 69–72.
7. Karami, K.; Ghasemi, M.; Naeini, N. H., *Catal. Commun.,* **2013**, *38*, 10–15.
8. Becke, A. D. *Phys. Rev. A* **1998**, *38*, 3098–3100.
9. Van Gisbergen, S. J. A.; Snijders, J. G.; Baerends, E. J.; *Comput. Phys. Commun.* **1999**, *118*, 119–138.
10. Frisch, M. J.; Trucks, G. W.; Schlegel, H. B.; Scuseria, G. E.; Robb, M. A.; Cheeseman, J. R.; Scalmani, G.; Barone, V.; Mennucci, B.; Petersson, G. A.; Nakatsuji, H.; Caricato, M.; Li, X.; Hratchian, H. P.; Izmaylov, A. F.; Bloino, J.; Zheng, G.; Sonnenberg, J. L.; Hada, M.; Ehara, M.; Toyota, K.; Fukuda, R.; Hasegawa, J.; Ishida, M.; Nakajima, T.; Honda, Y.; Kitao, O.; Nakai, H.; Vreven, T.; Montgomery, J. A., Jr.; Peralta, J. E.; Ogliaro, F.; Bearpark, M.; Heyd, J. J.; Brothers, E.; Kudin, K. N.; Staroverov, V. N.; Kobayashi, R.; Normand, J.; Raghavachari, K.; Rendell, A.; Burant, J. C.; Iyengar, S. S.; Tomasi, J.; Cossi, M.; Rega, N.; Millam, J. M.; Klene, M.; Knox, J. E.; Cross, J. B.; Bakken, V.; Adamo, C.; Jaramillo, J.; Gomperts, R.; Stratmann, R. E.; Yazyev, O.; Austin, A. J.; Cammi, R.; Pomelli, C.; Ochterski, J. W.; Martin, R. L.; Morokuma, K.; Zakrzewski, V. G.; Voth, G. A.; Salvador, P.; Dannenberg, J. J.; Dapprich, S.; Daniels, A. D.; Farkas, Ö.; Foresman, J. B.; Ortiz, J. V.; Cioslowski, J.; Fox, D. J. Gaussian 09, revision C.1; Gaussian, Inc.: Wallingford, CT, 2009.